Tonic feedback motor commands drive visuomotor learning

Yuto Makino[1,2,3*], Toshiki Kobayashi[2,3,4,5], Daichi Nozaki[2,6*]

[1] Center for Information and Neural Networks, National Institute of Information and Communications Technology, Osaka 565-0871, Japan

[2] Division of Physical and Health Education, Graduate School of Education, The University of Tokyo, Tokyo 113-0033, Japan

[3] Japan Society for the Promotion of Science, Tokyo 102-0083, Japan

[4] Sony Computer Science Laboratories, Tokyo 141-0022, Japan

[5] Integrated Open Systems Unit, Okinawa Institute of Science and Technology Graduate University, Okinawa 904-0495, Japan

[6] UTokyo Sports Science Initiative, The University of Tokyo, Tokyo 153-8902, Japan

*Corresponding authors: ymakino@nict.go.jp (YM); nozaki@p.u-tokyo.ac.jp (DN)

Abstract

When a movement error occurs, the motor system updates its commands to improve performance on subsequent trials. A prominent feedback error learning hypothesis proposes that the feedback response that corrects movement within a trial serves as a teaching signal for the learning response, observed as changes in motor commands on the next trial. However, how the temporal pattern of the feedback response influences the learning response remains unclear. Here, we introduce an experimental paradigm that directly compares the temporal patterns of feedback and learning responses across different patterns of visual error. We show that although the feedback response closely tracks the temporal pattern of the visual error, this temporal pattern is not transferred to the learning response. Instead, the amplitude of the feedback response during the holding period, reflecting the temporal pattern of the visual error, primarily determines the magnitude of the learning response. These findings reveal how the motor learning system selectively extracts specific components of feedback responses to update future motor commands.

Introduction

Accurate and consistent movements rely on the motor system's ability to correct movement errors. Motor adaptation, the process by which motor commands are updated based on sensory error information, has been extensively studied using perturbations during arm reaching tasks. In these paradigms, lateral deviations of the hand or cursor trajectory are typically treated as scalar measures of both motor commands and movement errors. This framework has enabled systematic investigation of key properties of motor adaptation, including the time course of adaptation and deadaptation [1], interference between opposing perturbations [2], generalization across targets [3-4], context dependency [5], and the presence of multiple timescales of motor memory [6].

Despite these advances, two fundamental questions remain. First, sensory error information is represented in sensory space rather than motor command space, and therefore cannot be directly used to update motor commands [7-9]. Second, treating motor commands as scalar values fails to capture their temporal dynamics. The feedback error learning hypothesis [9] has been proposed as a mechanism that addresses these issues. According to this hypothesis, the motor commands that correct a movement within a trial, referred to as feedback responses (FBRs), serve as teaching signals for updating motor commands expressed in subsequent trials, referred to as learning responses (LRs).

Albert and Shadmehr [10] provided behavioral evidence supporting this idea by comparing muscle activity during feedback responses in force field perturbation trials with learning responses in subsequent trials. They reported that learning responses resembled feedback responses temporally advanced by approximately 125 ms, and that larger feedback responses led to larger learning responses, suggesting that feedback responses may act as teaching signals. However, other studies have shown that feedback responses follow the

temporal characteristics of the perturbation, whereas such temporal features are not preserved in learning responses [11-12]. Moreover, our recent work [13] demonstrated a dissociation between feedback and learning responses when multiple or variable visual errors were imposed. Together, these findings challenge the notion that feedback responses universally serve as direct teaching signals.

Thus, a systematic reinvestigation of the relationship between feedback and learning responses is essential for understanding how feedback responses contribute to motor learning. To address this issue, we combined a single trial adaptation paradigm [3,10,13-15] with a force channel method originally developed to quantify feedback responses to visual errors [16-17]. This approach enables direct comparison of the temporal profiles and magnitudes of feedback and learning responses elicited by different visual error patterns, while minimizing changes in movement kinematics.

The present study aimed to elucidate how the motor system determines both the amplitude and temporal pattern of the learning response based on the feedback response. We addressed three questions. First, how does the learning response depend on the onset timing of the feedback response? Second, how does the amplitude of the feedback response influence the amplitude of the learning response? Third, how is the learning response shaped when the temporal pattern of the feedback response is drastically altered? Together, these questions allow us to dissociate which components of feedback responses contribute to the updating of future motor commands.

Results

Experimental paradigm to compare the FBR and LR

A total of 33 healthy participants took part in the study (Experiments 1–3). They were instructed

79 to move a visual cursor toward a frontal target by moving the handle of a robotic manipulandum
80 (KINARM). Each participant repeated a cycle consisting of three consecutive force channel
81 trials (baseline, perturbation, and probe trials) during which the handle trajectory was
82 constrained along the straight path [18], followed by two ordinary (i.e., without force channel)
83 reaching trials to washout the possible learning effect (Fig. 1a). In the baseline trial (Fig. 1b),
84 the lateral force exerted against the force channel was measured to determine a baseline force
85 when no perturbation was imposed on the cursor. In the subsequent perturbation trial (Fig. 1c),
86 the cursor position was shifted laterally either to the left or right (i.e., cursor shift perturbation;
87 [16-17]). The FBR was obtained as the lateral force induced by this cursor shift, subtracted by
88 the baseline force. In the following probe trial (Fig. 1d), the LR elicited by the preceding
89 perturbation was obtained as the lateral force, again subtracted by the baseline force. During
90 this probe trial, the cursor was invisible to prevent any online movement correction. For
91 analysis, the temporal profiles of FBR and LR were collapsed across rightward and leftward
92 cursor shift perturbations (Fig. 1e).

93 This experimental paradigm offers several advantages over conventional methods for
94 investigating the relationship between visual errors, FBRs, and LRs. First, the cursor shift
95 perturbation allowed us to impose arbitrary temporal patterns of visual errors by manipulating
96 the timing and magnitude of the cursor shift (Fig. 1c). Second, the temporal profiles of motor
97 commands associated with both FBR and LR could be directly compared, as they were derived
98 from forces measured against the force channel and were therefore not confounded by changes
99 in movement kinematics.

100

101 **Experiment 1: Effect of visual perturbation onset on the temporal profiles of FBR and LR**

102 The feedback error learning hypothesis proposes that FBRs serve as teaching signals for LRs.
103 Consistent with this idea, a previous study reported that LRs are time shifted versions of FBRs,

104 with a temporal advance of approximately 125 ms [10].

105 Experiment 1 (10 participants; seven men and three women) examined how the onset
106 timing of visual perturbations influences the relationship between the temporal profiles of FBRs
107 and LRs. In the perturbation trial, the cursor was shifted laterally by 3 cm either to the right or
108 left at different distances from the starting position (Fig. 2a; 1, 6, 11, and 16 cm). In addition,
109 one condition involved no cursor shift, resulting in a total of nine perturbation conditions (two
110 shift directions × four shift locations + one no shift condition).

111 Figure 2b shows the FBRs, obtained by subtracting the lateral forces measured during
112 the baseline trial from those measured during the perturbation trial. Although participants were
113 instructed not to use any explicit strategy, the cursor shift elicited implicit FBRs in the direction
114 opposite to the cursor shift, consistent with compensatory corrections. The latency of FBRs was
115 estimated using a receiver operator characteristic analysis [19-20]. This analysis revealed that
116 feedback responses emerged 155.9 ± 13.9 ms after the cursor shift onset, with no significant
117 differences across shift locations (Fig. 2c; $F(3,27) = 1.688$, $p = 0.193$, one-way repeated-
118 measures ANOVA). This latency is consistent with previous reports of rapid visually driven
119 feedback responses [17,21-23].

120 If LRs were fixed time shifted copies of FBRs [10], the onset of LRs should vary
121 systematically with the onset of FBRs, and their temporal profiles should closely match.
122 However, the lateral forces measured during the probe trial revealed a different pattern. Figure
123 2d illustrates the LRs, computed as the difference in lateral force between the probe and
124 baseline trials, showing that LRs consistently emerged just before movement onset, regardless
125 of the cursor shift location.

126 To quantify the temporal relationship between FBRs and LRs, we computed the cross-
127 correlation between the two responses (Fig. 2e). One-way repeated-measures ANOVA revealed

that the temporal shift corresponding to the maximum cross-correlation varied significantly with the perturbation onset location (Fig. 2f; $F(1.682, 15.135) = 11.341$, $p = 0.001$, Greenhouse Geisser correction). In contrast, Fisher transformed cross-correlation coefficients were significantly greater than zero for all perturbation conditions at the lag that maximized the correlation (Fig. 2g; 1 cm: $t(9) = 9.182$, $p < 0.001$; 6 cm: $t(9) = 8.956$, $p < 0.001$; 11 cm: $t(9) = 11.747$, $p < 0.001$; 16 cm: $t(9) = 8.380$, $p < 0.001$), indicating similar temporal profiles across responses. Together, these results indicate that although FBRs and LRs share similar temporal profiles, the relative timing between them is not fixed. Instead, LRs consistently emerge just before movement onset, independent of the onset timing of the FBRs.

Experiment 2: Effect of the size of visual error on the quantitative relationship between FBR and LR

In Experiment 1, the magnitude of the cursor shift was fixed at 3 cm while its onset location was varied. Experiment 2 (12 participants; six men and six women) examined how the magnitude of the cursor shift, while keeping its location constant, influenced FBRs and LRs. In the perturbation trials, the cursor was shifted laterally by 0.4, 0.8, 1.2, 1.6, 2.0, or 3.0 cm, all applied at a location 1 cm from the starting position (Fig. 3a).

Figure 3b illustrates the temporal patterns of FBRs across different cursor shift magnitudes. As observed in Figure 2, the FBRs consisted of an early phasic component followed by a later tonic component. Franklin et al. [23] reported that the magnitude of the FBR immediately after cursor shift onset is linearly modulated by the magnitude of the cursor shift. Consistent with this finding, the amplitude of the early phasic component increased systematically with increasing cursor shift magnitude. In contrast, the amplitude of the later tonic component, observed near movement offset, appeared to saturate when the cursor shift magnitude exceeded 0.8 cm. Figure 3c illustrates the temporal patterns of LRs across different

cursor shift magnitudes. In contrast to FBRs, the waveforms of LRs remained largely similar across conditions, while their amplitudes showed only modest modulation with cursor shift magnitude.

To further characterize how the temporal patterns of FBRs and LRs vary with error magnitude, we performed cross-correlation analyses for each cursor shift magnitude (Fig. 3d). This analysis revealed that the overall shape of the cross-correlation function changed systematically with error magnitude. To quantify these differences, we evaluated cross-correlation coefficients at two specific time lags between the FBRs and LRs: a fixed lag corresponding to the maximum cross-correlation observed in the 1 cm condition of Experiment 1 (Fig. 3e; -238 ms), and a longer lag of -500 ms (Fig. 3f). A two-way repeated-measures ANOVA revealed a significant interaction between time lag and error magnitude ($F(5,55) = 3.061$, $p = 0.017$). We then performed simple main effects analyses at each time lag. These analyses showed that the main effect of error magnitude was significant at the longer lag (Fig. 3f; -500 ms: $F(5,55) = 2.734$, $p = 0.028$), but not at the shorter lag (Fig. 3e; -238 ms: $F(5,55) = 0.891$, $p = 0.494$). This selective modulation of temporal similarity at longer lags indicates that the temporal profile of the FBR changes with increasing error magnitude, potentially reflecting the recruitment of distinct feedback-related components. In contrast, the temporal patterns of LRs remained relatively invariant across error magnitudes.

To quantitatively evaluate how response components vary with error magnitude, we decomposed the waveforms of the FBRs and LRs, [R(t)], into phasic and tonic components using the following equation (Figs. 4a, c):

$$\mathrm{R}(t) = \alpha \exp\left[-\frac{(t-T)^2}{2\sigma^2}\right] + \beta \int_0^t \frac{1}{\sqrt{2\pi\sigma^2}} \exp\left[-\frac{(\tau-T)^2}{2\sigma^2}\right] \mathrm{d}\tau, \quad (1)$$

where α, β, σ and T are constants. Note that α and β represent the amplitudes of early phasic and late tonic components, respectively. This formulation was inspired by previous studies

177 suggesting that motor commands during reaching consist of two components: a movement
178 related signal and a holding related signal, with the latter generated by integrating the former
179 over the course of the movement [24-25].

180 We first fitted the FBRs, aligned to the onset of the cursor shift and averaged across
181 participants, using Eq. 1. The fitted model accurately reproduced the experimentally observed
182 temporal patterns of the FBR (Fig. 4b, R^2= 0.9627, σ= 59, T =289). Assuming that the temporal
183 parameters of the model (σ and T) were approximately consistent across participants, we then
184 refitted the feedback responses for each individual while estimating only the amplitudes of the
185 phasic and tonic components. Notably, allowing the temporal parameters to vary freely did not
186 substantially affect the results reported below (Supplementary Figure. 1).

187 We applied the same analysis to the LRs aligned to movement onset, which yielded
188 similarly good fits (Fig. 4d; R^2= 0.961, σ= 126, T =118). Figures 4e and 4f show how the
189 amplitudes of the phasic and tonic components of both responses varied with error magnitude.
190 Consistent with the temporal patterns shown in Figs. 3b and 3c, the phasic component of the
191 FBR increased approximately linearly with error magnitude up to 1.8 cm. In contrast, the tonic
192 component of the FBR and both the phasic and tonic components of the LR saturated at
193 approximately 0.8 cm (Figs. 4e, f).

194 Based on the near linear scaling of the phasic FBR component and the early saturation
195 of the other components, we hypothesized that LRs would be more strongly driven by the tonic
196 component of the FBR. To test this hypothesis, we performed linear regression analyses using
197 the model $y = ax$, where x represents the amplitude of each FBR component and y represents
198 the corresponding component of the LR. As shown in Figure 4g, the phasic FBR component
199 exhibited only moderate predictive power (R^2 = 0.635 for the phasic LR component and R^2 =
200 0.698 for the tonic LR component). In contrast, when the tonic FBR component was used as

the predictor (Fig. 4h), both relationships were markedly stronger ($R^2 = 0.880$ for the phasic LR and $R^2 = 0.970$ for the tonic LR), indicating a higher degree of linearity. Together, these results indicate that the tonic component of the feedback response serves as the primary source of learning response modulation across different error magnitudes.

Experiment 3: Effect of biphasic temporal patterns of visual error on the FBR and LR

Although the phasic and tonic components of FBRs and LRs were differently modulated by error magnitude in Experiment 2, the overall temporal profiles of both responses remained largely similar across Experiments 1 and 2, regardless of cursor shift position or error magnitude. This similarity may reflect the use of stepwise cursor shift perturbations in both experiments, which limited the range of temporal patterns of visual error and may have constrained dissociation between the two responses.

To more directly test whether the temporal patterns of the FBR and LR could be dissociated, we introduced more complex temporal patterns of visual error in Experiment 3 (11 participants: six men and five women). Specifically, three different temporal patterns of cursor shift perturbation were employed (Fig. 5a). In all perturbation conditions, the cursor was first shifted laterally by ±3 cm at the 1 cm location. Following this first shift, the cursor position was either maintained (maintained condition), returned to its original position (removed condition), or shifted to the opposite side (reversed condition) (Fig. 5a). The second cursor shift, when present, occurred at one of three locations (6, 11, and 16 cm).

The temporal pattern of the LRs differs from that of the FBRs

Figures 5b–d illustrate the temporal profiles of the FBRs to cursor shift perturbations in Experiment 3. FBRs were sensitive not only to the initial cursor shift but also to the second shift. For example, when the second cursor shift occurred late in the movement at 16 cm, the

226 feedback responses during the movement period were nearly identical across conditions, with
227 differences emerging primarily during the holding period (Fig. 5b). As the second shift was
228 applied earlier in the movement, these differences became increasingly pronounced. Notably,
229 when the second shift occurred at 6 cm (Fig. 5d), the FBR returned to baseline in the removed
230 condition and became negative in the reversed condition.

231 In contrast to the FBRs, the LRs did not follow the temporal patterns of the cursor shift
232 perturbations (Figs. 5e–g) and therefore did not resemble the FBRs. For example, when the
233 second cursor shift occurred at 6 cm in the reversed condition, the biphasic pattern observed in
234 the FBR (Fig. 5d) differed markedly from the temporal profile of the LR (Fig. 5g). To quantify
235 this dissociation, we computed cross-correlation functions between the FBR and LR (Fig. 5h)
236 and assessed similarity using the cross-correlation coefficient at a fixed time lag (Fig. 5i). This
237 lag corresponded to the time yielding maximum cross-correlation in the 1 cm condition of
238 Experiment 1 and was used as a reference, as in Experiment 2.

239 As in Experiment 1, the cross-correlation coefficient in the maintained condition was
240 approximately 0.7, indicating moderate similarity between FBRs and LRs. However, this
241 similarity was significantly modulated by both the temporal structure of the second shift and its
242 location (Fig. 5i). Focusing on conditions where the second shift occurred at 16 cm, a one-way
243 repeated-measures ANOVA revealed a significant main effect of perturbation condition on the
244 cross-correlation coefficient ($F(2,20) = 3.633$, $p = 0.045$). Post hoc testing indicated that
245 similarity was significantly lower in the reversed condition than in the maintained condition
246 ($t(10) = 2.695$, $p = 0.042$, Holm-corrected). These results indicate that even when the second
247 shift occurred late in the movement, altering the temporal structure of the visual error reduced
248 the similarity between FBR and LR.

249 Focusing further on the removed and reversed conditions, a two-way repeated-measures

ANOVA revealed a significant interaction between error pattern and second shift location ($F(2,20) = 4.569$, $p = 0.023$). Post hoc tests showed significant main effects of both error pattern ($t(10) = 4.122$, $p = 0.002$, Holm-corrected) and shift location (11 cm vs. 16 cm: $t(10) = 2.784$, $p = 0.023$; 6 cm vs. 16 cm: $t(10) = 3.493$, $p = 0.007$, Holm-corrected). Together, these results provide strong evidence that the temporal pattern of the LR does not consistently resemble that of the FBR.

The modulation of the LR by the second shift is explained by the tonic components of the FBR

Focusing on conditions in which the second cursor shift was imposed at 16 cm, the FBRs were nearly identical during the movement period and diverged only slightly during the holding period (Fig. 5b). Despite this subtle difference, the amplitude of the LR in the subsequent trial differed markedly across conditions (Fig. 5e), consistent with the results of Experiment 2 and suggesting that the tonic component of the FBR plays a key role in determining LR amplitude. To quantify the coupling between FBRs and LRs attributable specifically to the second shift, we isolated its contribution by subtracting the FBRs and LRs in the maintained condition (no second shift) from those in the removed and reversed conditions (Figs. 6a–b, inset). We then fitted the decomposition model to these differential waveforms of the FBR and LR to test our hypothesis.

The decomposition model successfully reproduced the differential force profiles of both FBRs (Fig. 6a; $R^2 = 0.913$, $\sigma = 47$, T = 263) and LRs (Fig. 6b; $R^2 = 0.815$, $\sigma = 131$, T = 97). We next examined how the second cursor shift affected the phasic and tonic components of FBRs and LRs. Following the approach used in Experiment 2, we performed linear regression by using the model $y = ax$, where x represents the amplitude of each FBR component and y represents the amplitude of each component in the LR. As shown in Figure 6c, when FBR

amplitudes were used to predict LR amplitudes across second shift locations (6, 11, 16 cm), the phasic component exhibited poor prediction power (left panel, $R^2 = -0.208$), as did the tonic component (right panel, $R^2 = -0.040$). In contrast, when LRs were regressed against the tonic FBR amplitude (Fig. 6d), both the phasic (left panel, $R^2 = 0.978$) and tonic (right panel, $R^2 = 0.971$) components of the LR showed strong linear relationships. These findings indicate that the phasic FBR component does not reliably account for the LR. Instead, the tonic FBR component integrates the effects of both the first and second cursor shifts, and the summed magnitude of this tonic component determines the amplitude of the subsequent LR.

The tonic component of the FBR explains across-subject variability in the amplitude of the LR

In Experiments 1–3, we examined how LRs are generated through the utilization of FBRs. However, LRs could, in principle, be generated directly from visual error without relying on FBRs. Indeed, previous studies have shown that measurable LRs can occur even when only endpoint error is provided, in the absence of within-trial FBRs [13,15, 26-27],To directly test whether the tonic component of the FBR, rather than visual error itself, serves as the teaching signal for LR, it is necessary to compare FBRs and LRs under an identical temporal pattern of visual error. All participants in Experiments 1–3 (N = 33) experienced a cursor shift perturbation in which the cursor was laterally shifted 3 cm at the 1 cm location from the starting position (Fig. 7a). We therefore performed an additional analysis using this common temporal visual error pattern to examine whether across-subject variability in LR amplitude could be explained by the tonic component of the FBR.

Figures 7b and 7c show the temporal profiles of the FBR (Fig. 7b) and LR (Fig. 7c) elicited by visual errors of the identical magnitude. Participants who exhibited larger FBRs during the holding period tended to produce larger LRs. To quantify these individual

differences, we estimated the amplitudes of the FBRs and LRs by fitting their temporal profiles to the decomposition model (FBR: R^2= 0.9923, σ= 62, T = 300; LR: R^2= 0.9697, σ= 138, T = 136) and compared the extracted component amplitudes across participants. To directly assess whether individual differences in LR generation can be predicted from FBRs, we examined correlations between the amplitudes of the phasic and tonic components of the two responses (Figs. 7d-g). No significant correlation was observed between the phasic component of the FBR and either the phasic component of the LR (Fig. 7d; phasic, r = 0.224, p = 0.210) or tonic component of the LR (Fig. 7e; r = 0.052, p = 0.774). Similarly, the tonic component of the FBR did not correlate with the phasic component of the LR (Fig. 7f; r = -0.274, p = 0.123). In contrast, a strong and significant positive correlation was observed between the tonic components of the FBRs and LRs (Fig. 7g; r = 0.816, p < 0.001). Together, these results indicate that, at the level of individual differences, the tonic component of the FBR selectively predicts the amplitude of the tonic component of the LR. This finding further supports the hypothesis that the tonic FBR serves as a teaching signal for motor learning.

The tonic component of the FBR explains trial-by-trial variability in LR amplitudes

We next examined trial-by-trial variability in LR amplitudes. Even when the same visual error was applied, some trials elicited larger LRs whereas others elicited smaller ones. We tested whether this variability could be explained by the amplitude of the tonic component of the FBR using the data of the same condition in Experiments 1–3 (±3 cm cursor shift at the 1 cm location; N = 33). For each participant, trials were randomly divided into two datasets. These datasets were classified as High-FBR or Low-FBR based on the amplitude of the tonic component extracted from the averaged FBR. During this procedure, we ensured that the baseline trial force profiles were comparable between the two datasets, because differences in baseline force profiles can strongly influence the classification (see Methods). This random partitioning and

325 selection procedure was repeated 100 times for each participant, and the resulting High-FBR
326 and Low-FBR waveforms, as well as their corresponding LR waveforms, were obtained by
327 averaging 100 waveforms. The decomposition model (Eq. 1) was then applied to the averaged
328 waveforms to calculate the amplitudes of the phasic and tonic components of FBRs and LRs.

329 Figure 8a shows the force waveforms corresponding to the Low- and High-tonic FBR
330 components, averaged across all participants in Experiments 1–3 (N = 33). Clear differences
331 were observed during the late period between the two datasets, confirming successful
332 partitioning. Figure 8b summarizes the difference in the amplitudes of the phasic and tonic
333 components of the FBR between High- and Low- FBR datasets for all 33 participants. A one
334 sample t-test confirmed that this classification produced a significant difference only in the
335 tonic component (Fig. 8b; $t(32) = 8.737$, $p < 0.001$), with no significant difference in the phasic
336 component (Fig. 8b; $t(32) = 1.192$, $p = 0.242$). The corresponding temporal profiles of the LR
337 are shown in Figure 8c. A significant difference was observed in the amplitude of the tonic LR
338 component between the two datasets (Fig. 8d; $t(32) = 3.785$, $p < 0.001$), corresponding to an
339 average 16.76% reduction in tonic LR amplitude in the High-tonic FBR dataset relative to the
340 Low-tonic FBR dataset. In contrast, no significant difference was observed in the phasic
341 component of LR (Fig. 8d; $t(32) = 0.278$, $p = 0.783$). Importantly, these differences cannot be
342 attributed to differences in baseline force waveforms, as the force waveforms of the baseline
343 trials were comparable between the two datasets (Figs. 8a, c).

344 We next repeated this analysis by classifying trials based on the amplitude of the phasic
345 component of the FBR (Fig. 8e). As expected, this classification yielded significant differences
346 only in the phasic component of the FBR (Fig. 8f; $t(32) = 14.29$, $p < 0.001$), with no differences
347 in the tonic component (Fig. 8f; $t(32) = -0.349$, $p = 0.730$). However, classification based on
348 phasic FBR component produced little change in the temporal profile of the LR (Fig. 8g). No

349 significant difference was found in the amplitude of the tonic LR component between the two
350 datasets (Fig. 8d; $t(32) = -0.60$, $p = 0.55$, one-sample t-test). Although classification based on
351 the phasic FBR component yielded a small but statistically significant difference in overall LR
352 amplitude ($t(32) = 2.54$, $p = 0.016$), this effect was modest (6.15% change) and substantially
353 smaller than effect of the tonic-FBR–based classification on the tonic LR component (16.76%).
354 Together, these results demonstrate that trial-by-trial variability in LR is primarily explained
355 by the magnitude of the tonic component of the FBR, rather than by the phasic component.
356

357 # Discussion

358 Accurate movement relies on the motor system's ability to update motor commands across
359 trials based on sensory feedback about movement errors. A central unresolved question is how
360 the motor system utilizes the temporal structure of sensory error information to generate the
361 LR. According to the widely discussed feedback-error learning hypothesis [9], the FBRs
362 produced within a trial serve as teaching signals for generating LRs. Although this hypothesis
363 has received substantial support, it remains debated whether LRs are primarily constructed from
364 FBRs or instead directly from visual error information, and how these different sources
365 contribute to distinct features of the LR, such as its amplitude and temporal pattern.

366 To address these issues, we employed an experimental paradigm originally developed
367 to investigate FBRs [16]. This approach was well suited for our purpose, as it allowed direct
368 comparison of FBRs and LRs across a wide range of visual error patterns by measuring the
369 lateral forces generated against a clamp channel. Our experimental results demonstrate that the
370 motor system does not transfer the temporal profile of the FBR to the LR. Instead, it adjusts the
371 amplitude of the LR, whose temporal pattern remains relatively invariant, according to the
372 amplitude of the FBR, particularly the component that persists through the holding phase (i.e.,

373 tonic component). These findings clarify how the motor system selectively extracts specific
374 components of FBRs to update motor commands on subsequent trials.
375
376 **The LR is not a time-shifted version of the FBR**
377 A fundamental problem in motor control is how the motor system updates motor commands in
378 response to movement errors. This updating process is nontrivial because the error information
379 is represented in the sensory space and must be transformed into motor commands. The
380 feedback error learning hypothesis offers an elegant solution to this problem by proposing that
381 the FBR to a movement error—namely, the motor commands used to correct the error within a
382 trial—serves as a teaching signal for generating the LR, expressed as updated motor commands
383 in the subsequent trial.

384 A direct prediction of this hypothesis is that the LR should resemble a time-shifted
385 version of the FBR. Supporting this view, Albert and Shadmehr [10] reported that, under a
386 velocity-dependent force-field perturbation, the LR closely matched a fixed time-shifted copy
387 of the FBR. They suggested that the magnitude of this time shift, approximately 125 ms, reflects
388 the sensorimotor delay required for the motor system to generate the FBR in response to
389 movement errors. However, because their study examined only a single type of force-field
390 perturbation, it remains unclear whether the motor system truly shifts the temporal profile of
391 the FBR forward in time based on sensory processing delays.

392 Addressing this question requires systematic manipulation of error timing. Fine and
393 Thoroughman [11] pursued this approach by applying brief force pulses at different positions
394 along the reaching trajectory. They found that FBRs emerged with a short latency after
395 perturbation onset, whereas LRs in the subsequent trial consistently appeared near movement
396 onset, largely independent of perturbation timing. However, the range of onset timings tested

397 in that study was relatively narrow (approximately 200 ms), and both FBRs and LRs were
398 inferred from movement trajectories, which may not sensitively reflect changes in underlying
399 motor commands. These methodological constraints may have obscured differences in
400 responses to force pulses applied at different times.

401 In the present study, we combined cursor-shift perturbations with an error-clamp
402 method, allowing visual errors to be imposed precisely while minimizing changes in movement
403 kinematics and avoiding secondary errors induced by FBRs or LRs themselves. This approach
404 enabled direct comparison of the temporal profiles of the visual errors, FBRs, and LRs (Fig. 1).
405 By systematically manipulating the onset of the cursor shift (Experiment 1), we found that the
406 temporal relationship between FBRs and LRs was not fixed (Fig. 2f). Even when visual error
407 onset varied widely—from shortly after movement onset to just before movement offset—the
408 LR consistently emerged before the movement onset. Consistent with the findings of Fine and
409 Thoroughman [11], these results demonstrate that the LR does not preserve temporal
410 information about when the error occurred and therefore cannot be considered not a fixed time-
411 shifted copy of the FBR.

412 Notably, this lack of temporal specificity in the learning response contrasts with
413 classical forms of cerebellar associative learning, such as delay eyeblink conditioning, in which
414 the cerebellum acquires precise timing relationships between conditioned and unconditioned
415 stimuli [28]. Moreover, recent work in mice has demonstrated temporally specific adaptation
416 and aftereffects depending on the position of mossy fiber stimulation during reaching
417 movements [29], where stimulation acts as an unconditioned signal. The temporal specificity
418 observed in these paradigms differs markedly from the present findings in human visuomotor
419 adaptation. Further studies will be required to clarify which cerebellar mechanisms distinguish
420 temporally precise associative learning from the form of adaptation examined here.

421

422 **Nonlinear modulation of the LR with error size reflects the tonic component of the FBR**

423 Experiment 2 examined the quantitative relationship between error magnitude and both FBRs
424 and LRs by systematically manipulating the magnitude of visual errors. Previous studies have
425 shown that the LR amplitude increases approximately linearly for small errors but saturates for
426 larger errors [30-33]. Several studies have also reported differential modulation of FBR and LR
427 by error magnitude [11, 13, 34]. However, in most of these studies, the visual error experienced
428 by participants could change during the movement as a consequence of the FBR itself,
429 complicating precise characterization of the temporal evolution of the FBR.

430 The cursor-shift perturbation paradigm, which imposes a constant visual error
431 throughout the movement [16], is therefore particularly well suited for examining how error
432 magnitude modulates FBRs and LRs. Using this approach in Experiment 2, we found that FBRs
433 were more sensitive to changes in error magnitude than LRs (Figs. 3b–c). Notably, consistent
434 with findings using brief (approximately 250 ms) cursor-shift perturbations (Franklin et al.
435 2016), this heightened sensitivity was confined to the early component of the FBR and was
436 largely absent in the late component.

437 Motivated by previous work suggesting that motor commands can be decomposed into
438 phasic and tonic components [25] or into velocity- and position-dependent components [24],
439 we decomposed both FBRs and LRs into two analogous components and examined how each
440 scaled with error magnitude (Figs. 4a–d). The phasic component of the FBR increased
441 approximately linearly with error magnitude up to 2.0 cm (Fig. 4e), whereas the other three
442 components—the tonic FBR and both components of the LR—exhibited similar nonlinear
443 modulation, saturating even at small error magnitudes (Figs. 4e–h). Because our paradigm
444 enabled full temporal profiling of both FBRs and LRs, we were able to identify these

445 component specific scaling relationships directly.

446 Although numerous computational models have been proposed to account for the
447 nonlinear modulation of LR amplitude with error magnitude [13, 30-33], our findings suggest
448 that such nonlinearities already emerge during the later phase of the FBR. The close
449 correspondence between the tonic FBR and LR supports the view that these responses share
450 partially overlapping neural computations, consistent with previous experimental and modeling
451 studies [34, 35-36].

452

453 **LRs differ from FBRs in temporal pattern and vary primarily in amplitude**

454 The temporal profiles of FBRs and LRs in Experiments 1 and 2 showed partial similarity,
455 consistent with the findings of Albert and Shadmehr [10]. However, this similarity may reflect
456 the use of simple step-like cursor shift perturbations, which impose limited temporal structure
457 on the visual error. In contrast, Wei et al. [12] examined a broader range of force perturbations
458 and evaluated FBRs and LRs using movement kinematics. They reported that FBRs exhibited
459 temporally specific corrections that closely followed the time course of the applied force,
460 whereas LRs displayed relatively nonspecific temporal profiles. However, because their
461 analyses relied on movement trajectories, it was not possible to isolate the temporal evolution
462 of the underlying motor commands or the sensory error from the corrective forces generated
463 during movement.

464 As described above, our experimental paradigm avoids these confounds by imposing
465 temporally precise visual errors while constraining movement kinematics, thereby enabling
466 direct comparison of the motor commands underlying FBRs and LRs. When visual
467 perturbations containing double cursor shifts were introduced in Experiment 3 (Fig. 5a), FBRs
468 closely track the temporal structure of the imposed error. In contrast, LRs neither reflected the

469 temporal pattern of the visual error nor resembled the temporal profile of the FBR (Figs. 5b–d).
470 Instead, the motor system generated a temporally nonspecific LR that emerged immediately
471 before movement onset (Figs. 5e–g). These results provide strong evidence that LRs do not
472 inherit the temporal structure of FBRs, but instead differ primarily in amplitude. This finding
473 extends and strengthens the conclusions of Wei et al. [12] by demonstrating this dissociation at
474 the level of motor commands rather than inferred kinematics.

475

476 **Modulation of LR amplitude according to the tonic component of the FBR**

477 The results of Experiment 2 support the idea that the tonic component of the FBR plays a central
478 role in determining the amplitude of the LR. This conclusion is strongly supported by three
479 complimentary analyses. First, inter-individual differences in LR magnitude were significantly
480 correlated only with the amplitude of the tonic component of the FBR (Fig. 7), consistent with
481 the previous findings of Albert and Shadmehr [10], who examined EMG activity associated
482 with FBRs and LRs. Second, trial-by-trial variability in LR amplitude was explained by the
483 tonic component of the FBR, but not by the phasic component (Fig. 8). Third, in Experiment 3,
484 the amplitude of the LR induced by the second cursor shift was also predicted by the amplitude
485 of the tonic component of the FBR evoked by the second cursor shift (Fig. 6).

486 Recent work suggests that the tonic component sustained until movement offset reflects
487 an integrated motor command accumulated over the course of the movement [25]. Albert and
488 colleagues [25] demonstrated an integrative linkage between moving and holding commands,
489 showing that the time integral of movement-related force persists into the holding period and
490 contributes to postural control. Similar integration mechanisms have been identified across
491 multiple neural systems. In the oculomotor system, sustained neural activity following saccade
492 termination has been attributed to a neural integrator that accumulates transient movement-

493 related signals to maintain gaze [37-38]. In spatial navigation, neurons in the medial entorhinal
494 cortex integrate velocity and directional inputs over time to estimate position [39-40]. Across
495 systems, such integrative mechanisms transform temporally distributed signals, such as velocity,
496 into representations of the current state [37]. In this framework, the feedback controller may
497 integrate the feedback response itself, which reflects the temporal pattern of sensory error, to
498 infer the state of the environment. The resulting tonic FBR then serves as a teaching signal that
499 sets the amplitude of the LR on the subsequent trial.
500

501 **Perspectives for future studies**

502 Despite the present findings, important aspects of how LRs are generated remain unresolved.
503 First, the temporal structure of the visual error used in this study was relatively simple,
504 consisting of linear combinations of stepwise cursor shifts. It remains to be determined whether
505 the relationship between the tonic component of the FBR and the amplitude of the LR
506 generalizes to more complex structures—such as nonlinear, nonstationary, or stochastic
507 perturbations. Establishing the reproducibility of this mechanism across a broader class of error
508 dynamics will be essential for evaluating its generality.

509 Second, the temporally nonspecific nature of the LR observed in the present study does
510 not fully account for previous findings showing that the motor system can acquire complex,
511 time-varying motor commands, such as those required to adapt to S-shaped force perturbations
512 [25, 41]. How trial-by-trial updating of motor commands gives rise to such structured LRs
513 under more dynamic conditions remains an important open question.

514 Finally, the present study does not address learning mechanisms that operate in the
515 absence of online FBRs. It is well established that endpoint (terminal) visual feedback can
516 induce LRs without engaging FBRs during the movement [10, 13, 26-27], and that motor

imagery can also drive learning in response to visual error [42]. Although endpoint error is generally considered a task error rather than a sensory prediction error and therefore engage reinforcement like mechanisms distinct from error-based adaptation [43-44], an important challenge for future work will be to clarify how LRs are generated from these fundamentally different sources of error.

Summary

In summary, we identified a mechanism by which the visuomotor learning system transforms visual error information into learning responses through the feedback responses. To elucidate this mechanism, we redesigned the experimental paradigm to enable direct comparison of the temporal profiles of feedback responses and learning responses across multiple patterns of visual error. Our results show that the motor system does not transfer the temporal structure of the feedback response to the learning response. Instead, the amplitude of the tonic component of the feedback response—which reflects the temporal history of the visual error—determines the magnitude of the learning response. Moreover, the amplitude of this tonic component accounted for both inter-individual and trial-by-trial variability in learning response amplitude. These findings provide a mechanistic framework for understanding how the motor learning system selectively extracts information from feedback responses to update motor commands.

Methods

General experimental procedures

A total of thirty-four right-handed participants (20 men and 14 women; age range, 18–40 years) volunteered to take part in the study. Each participant completed one of the three experiments. Participants were recruited using an online recruitment system (https://www.jikken-baito.com).

541 All participants provided written informed consent prior to participation, and all experimental
542 procedures were approved by the Office for Life Science Research Ethics and Safety of the
543 University of Tokyo.

544 Participants performed planar reaching movements with their right hand while holding
545 the handle of a robotic manipulandum (KINARM End-Point Lab, Kinarm, Kingston, Canada).
546 A horizontal screen positioned above the handle displayed a starting position, a target (5 mm
547 in diameter), and a white cursor (5 mm in diameter) indicating the handle position. This screen
548 occluded direct vision of the participant's arm and the handle.

549 The target was displayed 20 cm directly in front of the starting position. Approximately
550 one second after the participant placed the handle at the starting position, the target changed
551 color to magenta, serving as the "go" cue. Participants were instructed to move the handle
552 smoothly and as straight as possible toward the target and to avoid using explicit strategies,
553 even when the cursor was perturbed. The cursor disappeared 700 ms after movement
554 completion (i.e., during the holding period), and the handle was automatically returned to the
555 starting position. Participants were instructed to hold the handle at the perceived location of the
556 target and to refrain from moving during the holding period.

557 To maintain consistent movement speed across trials, feedback on peak velocity was
558 provided at the end of each trial: "too fast" (> 750 mm/s), "rather fast" (> 650 mm/s), "rather
559 slow" (< 450 mm/s), or "slow" (< 350 mm/s). Before the main experiment, participants
560 completed 50 practice trials to stabilize their movement accuracy and velocity.
561

562 **Experiment 1: Effect of visual perturbation onset on the LR**

563 In Experiment 1 (10 participants: seven men and three women), we employed a single-trial
564 visuomotor adaptation paradigm using a visual cursor-shift perturbation originally developed

565 to investigate FBRs [16]. In perturbation trials, the cursor was shifted laterally by ±3 cm at one
566 of four distances from the starting position (Fig. 2a; 1, 6, 11, and 16 cm). A baseline condition
567 with no cursor shift was also included. Each perturbation trial was flanked by channel trials
568 (Fig. 1a). During both perturbation and channel trials, hand trajectories were constrained to a
569 straight path from the starting position to the target using a clamp-channel method [18],
570 allowing measurement of the lateral force exerted against the channel. The force channel was
571 implemented using a virtual spring (6000 N/m) and damper [100 N/(m/s)].

572 The temporal profile of the FBR was quantified as the difference in the lateral force
573 between the perturbation and baseline trials, whereas the LR was quantified as the difference
574 between the probe and baseline trials [10], During probe trials, the cursor was removed to assess
575 the LR in the absence of visual feedback.

576 Each trial set consisted of five consecutive trials: a baseline trial to measure the baseline
577 lateral force profile, a perturbation trial (one of nine conditions: 4 positions × 2 shift directions
578 + 1 no shift condition), a probe trial (Fig. 1a), and two null trials without force channel or cursor
579 perturbation to wash out adaptation effects. One cycle comprising all nine perturbation types
580 was repeated 26 times. Including 50 practice trials, the total number of trials was 1,220 (50
581 practice trials + 5 trials × 9 perturbations × 26 cycles).
582

583 **Experiment 2: Effect of the visual error magnitude on the LR**

584 Experiment 2 (12 participants: six men and six women) examined the quantitative relationship
585 between FBRs and LRs across different magnitudes of cursor-shift perturbations. Participants
586 repeatedly performed a set consisting of five trials. In perturbation trials, the cursor was shifted
587 laterally by ±0.4, 0.8, 1.2, 1.6, 2.0, or 3.0 cm at a position 1 cm from the starting position (Fig.
588 3a). After 50 practice trials, one cycle comprising all 12 perturbation types was repeated 18

589 times, resulting in a total of 1,130 trials (50 practice trials + 5 trials × 12 perturbations × 18
590 cycles). One participant terminated the experiment early after completing 973 trials; for this
591 participant, only the first 15 cycles were included in the analysis.
592

593 **Experiment 3: Effect of the complex temporal patterns of visual error on the FBR and**
594 **LR**

595 Experiment 3 (12 participants: seven men and five women) examined whether different
596 temporal patterns of visual perturbations induce distinct patterns of FBRs and LRs. As in
597 Experiments 1 and 2, participants repeatedly performed a set consisting of five trials. In the
598 perturbation trials, three types of temporal perturbation patterns were used (Fig. 5a). In the
599 maintained conditions, the cursor was shifted by ±3 cm at a location 1 cm from the starting
600 position and the shift was maintained throughout the movement (2 types; +3cm or -3cm). In the
601 removed conditions, the cursor was shifted by ±3 cm at the 1 cm location and then returned to
602 zero (±3 cm → 0 cm) at one of three locations (6, 11, or 16 cm; 6 types). In the reversed
603 conditions, the cursor was shifted by ±3 cm at the 1 cm location and then reversed (±3 cm →
604 ∓3 cm) at one of the three locations (6, 11, or 16 cm; 6 types). In total, fourteen perturbation
605 types were used. After 50 practice trials, one cycle comprising all 14 types was repeated 18
606 times, yielding 1,310 trials (50 practice trials + 5 trials × 14 perturbations × 18 cycles). One
607 participant reported using an explicit strategy during the task and was therefore excluded from
608 all analyses.
609

610 **Data analysis**

611 Handle position and force data were sampled at 1000 Hz and low-pass filtered using a 4th-order
612 zero-lag Butterworth filter with a cutoff frequency of 6 Hz. Handle velocity was calculated by
613 numerically differentiating the position signal. The temporal profile of the FBR was defined as

614 the difference between lateral force profiles measured during the perturbation and baseline trials,
615 whereas the temporal profile of the LR was defined as the difference between lateral force
616 profiles measured during the probe and baseline trials.
617
618 *Cross-correlation analysis*
619 Temporal similarity and relative timing between FBRs and LRs were evaluated using cross-
620 correlation analysis. In Experiment 1, within-subject cross-correlations were computed to
621 determine the time lag that maximized the correlation between the two responses. For
622 Experiments 2 and 3, similarity was quantified using the cross-correlation coefficient at a fixed
623 time lag corresponding to the peak of the averaged cross-correlation function obtained in
624 Experiment 1 (cursor shift at 1 cm). In Experiment 2, cross-correlation coefficients were
625 additionally computed at a longer fixed lag of -500 ms to assess differences in the overall shape
626 of the cross-correlation functions.
627
628 *Onset detection using ROC analysis*
629 A receiver-operating characteristic (ROC) analysis was used to determine the onset latency of
630 the FBR (Green & Swets, 1974; Nashed et al., 2014). ROC curves were constructed to quantify
631 the probability of discriminating FBRs elicited by leftward versus rightward cursor shifts, with
632 force profiles aligned to the onset of the cursor shift. The discrimination point was defined as
633 the earliest time at which the ROC value exceeded 0.75 for at least 5 ms. To estimate the onset
634 at which the ROC curve began to deviate from chance (0.5), we regressed the ROC values
635 within the 15 ms window preceding the discrimination point and calculated the time at which
636 this regression line intersected the baseline of the ROC curve.
637
638 *Decomposition analysis*

To quantitatively characterize FBRs and LRs, we fitted their temporal profiles using Eq. 1. FBRs were aligned to the cursor-shift onset (Fig. 3a), whereas LRs were aligned to movement onset (Fig. 3b). Model fitting was first performed on response profiles averaged across participants to identify the parameters σ and T. Using these parameters, individual response profiles were then refitted to estimate the amplitudes of the phasic and tonic components. The same procedure was applied to FBRs and LRs elicited by the second cursor shift in Experiment 3. Specifically, the decomposition model was fitted to differential feedback response waveforms, computed as the difference between the removed or reversed conditions and the maintained condition, and aligned to the onset of the second shift (Fig. 6a, inset). An analogous analysis was performed for differential learning response waveforms aligned to movement onset (Fig. 6b, inset).

Linear regression relating FBR and LR amplitudes

To quantify the relationship between the phasic and tonic components of the FBR and LR, we performed linear regression using the model $y = ax$, where x represents the amplitude of each FBR component and y represents the amplitude of the corresponding LR component. Model performance was evaluated using the coefficient of determination (R^2) calculated between predicted and observed LR amplitudes. R^2 values were computed across all perturbation conditions to evaluate how well the phasic and tonic components of the FBR accounted for modulation of the corresponding components of the LR.

Dividing trials into Low and High tonic or phasic FBR components

Even when identical cursor shift magnitudes were applied, both FBRs and LRs exhibited substantial trial-by-trial variability. We therefore examined whether variability in the FBR was systematically related to variability in the LR. To this end, we analyzed trials from the same

condition in Experiments 1-3 (±3 cm cursor shift at 1 cm location; N = 33) and divided them into two datasets based on whether they exhibited larger tonic or phasic FBR components. For each participant, trials with rightward and leftward cursor shifts were randomly split into two datasets, and baseline force profiles, FBRs, and LRs were obtained for each dataset by collapsing force waveforms across cursor shift directions.

A critical issue in this classification procedure was that differences in baseline force profiles could strongly influence both FBRs and LRs. Because FBRs and LRs were computed by subtracting baseline force waveforms from the perturbed and probe trial waveforms, respectively, large differences in baseline force between datasets could lead to classification driven by baseline force variability rather than by genuine differences in FBRs. In such cases, both the FBRs and LRs waveforms would be contaminated by baseline force differences. To mitigate this problem, we repeated the random trial partitioning procedure 100 times and selected the pair of datasets that exhibited the highest similarity between baseline force profiles, defined as the smallest mean squared difference between baseline force profiles. This approach ensured that subsequent comparisons primarily reflected variability in feedback responses rather than differences in baseline force (see Figs. 8a, 8c, 8e and 8g).

We then fitted the FBR waveforms averaged within each dataset using Eq. 1 to estimate the amplitude of the phasic and tonic components. Based on the amplitude of either the phasic or tonic component of the FBR, each dataset was classified as a Low-phasic (or tonic) FRB or High-phasic (or tonic) FBR dataset. This procedure was repeated 100 times, and the baseline force, FBR and LR waveforms were averaged across repetitions for each Low and High FBR datasets. Finally, the grand averaged waveforms were again fitted using Eq. 1 to estimate the phasic and tonic components of both FBRs and LRs.

Data exclusion

We excluded the data from the analysis by the following criteria. The lateral force data in each cycle was discarded when the peak movement velocity for either a baseline trial, a perturbation trial, or a probe trial was outside the included range (< 450 mm/s or >750 mm/s). The proportion of the excluded cycle was 2.52% (Experiment 1), 2.70 % (Experiment 2), and 3.25 % (Experiment 3).

Acknowledgments

We thank members of the Nozaki Laboratory for their helpful comments and suggestions, as well as for their assistance in coordinating the experiments. This study was supported by grants from the Japan Society for the Promotion of Science (JSPS) Research Fellowships for Young Scientists (22KJ0992) to YM, JSPS KAKENHI (20J13734, 23K10739) to TK and JSPS KAKENHI (21H04860, 22K19736, 23K27958) to DN.

Author contributions

Conceptualization, Methodology, Formal analysis, Investigation, and Writing: Y.M., T.K., D.N.; Experimental setup: Y.M.; Supervision: D.N.

Declaration of Interest

The authors declare no competing interests.

Data availability

The source Matlab data that support the findings of this study and the programming codes to analyze the data are available in Zenodo (10.5281/zenodo.18297833), and raw experimental data is available from the corresponding author upon reasonable request.

References

1. Taylor JA, Ivry RB. Flexible cognitive strategies during motor learning. PLoS Comput Biol. 2011;7(3):e1001096.
2. Herzfeld DJ, Vaswani PA, Marko MK, Shadmehr R. A memory of errors in sensorimotor learning. Science. 2014;345:1349-1353.
3. Thoroughman KA, Shadmehr R. Learning of action through adaptive combination of motor primitives. Nature. 2000;407:742-747.
4. Donchin O, Francis JT, Shadmehr R. Quantifying generalization from trial-by-trial behavior of adaptive systems that learn with basis functions: theory and experiments in human motor control. J Neurosci. 2003;23:9032-9045.
5. Nozaki D, Kurtzer I, Scott SH. Limited transfer of learning between unimanual and bimanual skills within the same limb. Nat Neurosci. 2006;9:1364-1366.
6. Smith MA, Ghazizadeh A, Shadmehr R. Interacting adaptive processes with different timescales underlie short-term motor learning. PLoS Biol. 2006;4(6):e179.
7. Jordan MI, Rumelhart DE. Forward models: supervised learning with a distal teacher. Cogn Sci. 1992;16:307-354.
8. Jordan MI. Learning inverse mappings using forward models. In: Proceedings of the Sixth Yale Workshop on Adaptive and Learning Systems; 1990. p. 146-151.
9. Kawato M, Furukawa K, Suzuki R. A hierarchical neural-network model for control and learning of voluntary movement. Biol Cybern. 1987;57:169-185.
10. Albert ST, Shadmehr R. The neural feedback response to error as a teaching signal for the motor learning system. J Neurosci. 2016;36(17):4832-4845.
11. Fine MS, Thoroughman KA. Motor adaptation to single force pulses: sensitive to direction but insensitive to within-movement pulse placement and magnitude. J

Neurophysiol. 2006;96(2):710-720.

12. Wei K, Wert D, Körding K. The nervous system uses nonspecific motor learning in response to random perturbations of varying nature. J Neurophysiol. 2010;104(6):3053-3063.

13. Makino Y, Hayashi T, Nozaki D. Divisively normalized neuronal processing of uncertain visual feedback for visuomotor learning. Commun Biol. 2023;6:1396.

14. Castro LNG, Hadjiosif AM, Hemphill MA, Smith MA. Environmental consistency determines the rate of motor adaptation. Curr Biol. 2014;24:1050-1061.

15. Hayashi T, Kato Y, Nozaki D. Divisively normalized integration of multisensory error information develops motor memories specific to vision and proprioception. J Neurosci. 2020;40(7):1560-1570.

16. Franklin DW, Wolpert DM. Specificity of reflex adaptation for task-relevant variability. J Neurosci. 2008;28:14165-14175.

17. Dimitriou M, Wolpert DM, Franklin DW. The temporal evolution of feedback gains rapidly update to task demands. J Neurosci. 2013;33:10898-10909.

18. Scheidt RA, Reinkensmeyer DJ, Conditt MA, Rymer WZ, Mussa-Ivaldi FA. Persistence of motor adaptation during constrained, multi-joint, arm movements. J Neurophysiol. 2000;84:853-862.

19. Green DM, Swets JA. Signal detection theory and psychophysics. Oxford: Robert E. Krieger; 1974.

20. Nashed JY, Crevecoeur F, Scott SH. Rapid online selection between multiple motor plans. J Neurosci. 2014;34(5):1769-1780.

21. Scott SH. A functional taxonomy of bottom-up sensory feedback processing for motor actions. Trends Neurosci. 2016;39(8):512-526.

22. Day BL, Lyon IN. Voluntary modification of automatic arm movements evoked by

motion of a visual target. Exp Brain Res. 2000;130(2):159-168.

23. Franklin DW, Reichenbach A, Franklin S, Diedrichsen J. Temporal evolution of spatial computations for visuomotor control. J Neurosci. 2016;36:2329-2341.

24. Sing GC, Joiner WM, Nanayakkara T, Brayanov JB, Smith MA. Primitives for motor adaptation reflect correlated neural tuning to position and velocity. Neuron. 2009;64(4):575-589.

25. Albert ST, Hadjiosif AM, Jang J, Zimnik AJ, Soteropoulos DS, Baker SN, et al. Postural control of arm and fingers through integration of movement commands. eLife. 2020;9:e52507.

26. Wei K, Körding K. Uncertainty of feedback and state estimation determines the speed of motor adaptation. Front Comput Neurosci. 2010;4:11.

27. Burge J, Ernst MO, Banks MS. The statistical determinants of adaptation rate in human reaching. J Vis. 2008;8(4):20. doi: 10.1167/8.4.20.

28. Lavond DG, Knowlton BJ, Steinmetz JE, Thompson RF. Classical conditioning of the rabbit eyelid response with a mossy-fiber stimulation CS: II. Lateral reticular nucleus stimulation. Behav Neurosci. 1987;101:676-682.

29. Calame DJ, Becker MI, Person AL. Cerebellar associative learning underlies skilled reach adaptation. Nat Neurosci. 2023;26:1068-1079.

30. Wei K, Körding K. Relevance of error: What drives motor adaptation? J. Neurophysiol. 2009:101, 655–664.

31. Marko MK, Haith AM, Harran MD, Shadmehr R. Sensitivity to prediction error in reach adaptation. J Neurophysiol. 2012;108:1752-1763.

32. Kim HE, Morehead JR, Parvin DE, Moazzezi R, Ivry RB. Invariant errors reveal limitations in motor correction rather than constraints on error sensitivity. Commun Biol. 2018;1:19.

33. Tsay JS, Avraham G, Kim HE, Parvin DE, Wang Z, Ivry RB. The effect of visual uncertainty on implicit motor adaptation. J Neurophysiol. 2021;125:12-22.

34. Hayashi T, Yokoi A, Hirashima M, Nozaki D. Visuomotor map determines how visually guided reaching movements are corrected within and across trials. eNeuro. 2016;3(3):ENEURO.0032-16.2016.

35. Maeda RS, Cluff T, Gribble PL, Pruszynski JA. Feedforward and feedback control share an internal model of the arm's dynamics. J Neurosci. 2018;38(49):10505-10514.

36. Maeda RS, Gribble PL, Pruszynski JA. Learning new feedforward motor commands based on feedback responses. Curr Biol. 2020;30(10):1941-1948.e3.

37. Shadmehr R. Distinct neural circuits for control of movement vs. holding still. J Neurophysiol. 2017;117(4):1431-1460.

38. Robinson DA. Models of the saccadic eye movement control system. Kybernetik. 1973;14:71-83.

39. McNaughton BL, Battaglia FP, Jensen O, Moser EI, Moser MB. Path integration and the neural basis of the “cognitive map.” Nat Rev Neurosci. 2006;7:663-678.

40. Burak Y, Fiete IR. Accurate path integration in continuous attractor network models of grid cells. PLoS Comput Biol. 2009;5(2):e1000291.

41. 40. Makino Y, Suemitsu K, Hirashima M. Action progress organizes motor memory. bioRxiv [Preprint]. 2026 [posted 2026 Feb 9; cited 2026 Mar 19]. Available from: https://www.biorxiv.org/content/10.64898/2026.02.09.704807v1
doi: 10.64898/2026.02.09.704807

42. Kim OA, Forrence AD, McDougle SD. Motor learning without movement. Proc Natl Acad Sci U S A. 2022;119(30):e2204379119.

43. Ikegami T, Ganesh G, Gibo TL, Yoshioka T, Osu R, Kawato M. Hierarchical motor adaptations negotiate failures during force field learning. PLoS Comput Biol.

2021;17(4):e1008481.

44. Kim HE, Parvin DE, Ivry RB. The influence of task outcome on implicit motor learning. eLife. 2019;8:e39882.

Figures

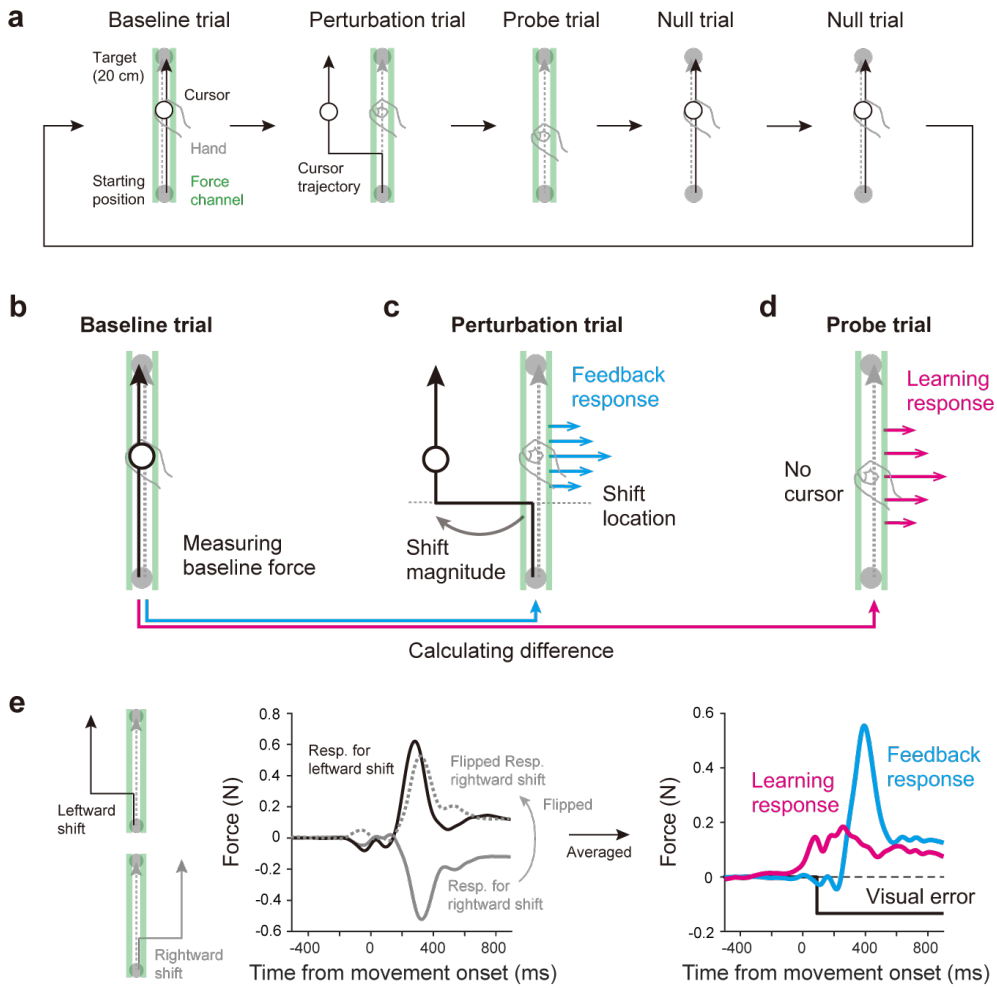

Figure 1: Procedures of the experimental paradigm. We employed a cursor shift perturbation paradigm to reinvestigate the relationship between feedback responses (FBRs) and learning responses (LRs). **A,** Participants repeatedly performed a block consisting of one baseline trial, one perturbation trial, one probe trial followed by two null trials. **B,** Baseline trials. Forces exerted against the force channel were measured to quantify baseline motor output. **C,** In perturbation trials, the cursor was shifted laterally by manipulating both location and magnitude of the shift. This manipulation allowed the imposition of arbitrary temporal patterns of visual error. Hand trajectories were constrained using the force channel. **D,** Probe trials were used to measure the LR elicited for the visual error imposed in the preceding perturbation trial. Temporal patterns of FBRs and LRs were baseline-subtracted using forces measured during baseline trials. **E,** Temporal profiles of responses to rightward and leftward cursor shift perturbations were collapsed (left) to enable direct comparison of the motor commands underlying FBRs and LRs for a given temporal pattern of visual error.

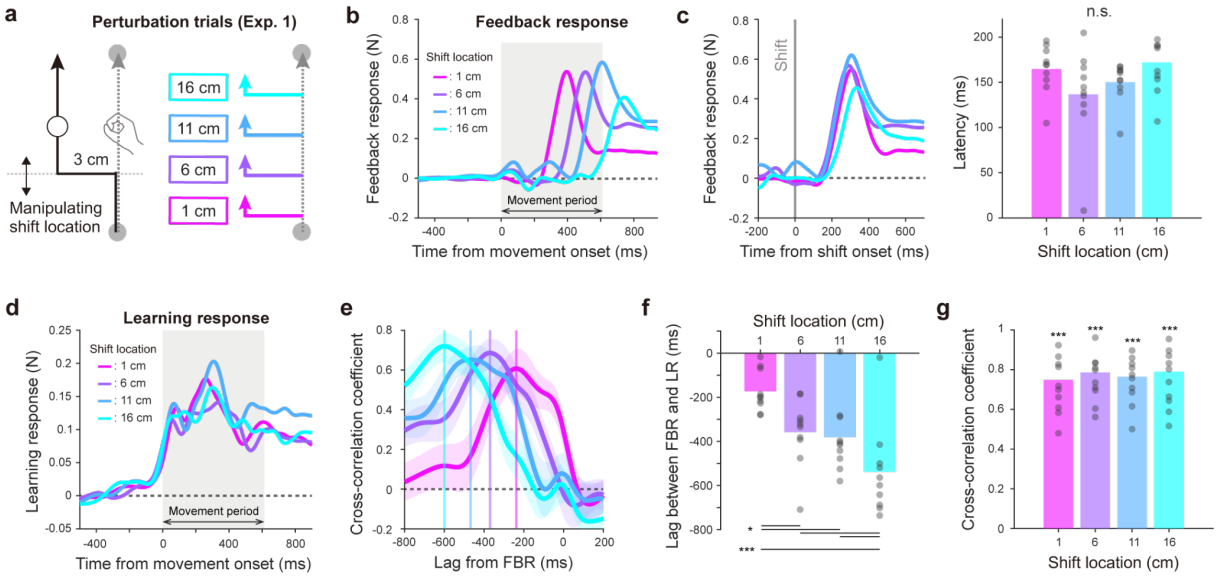

Figure 2: Relationship between feedback and learning responses in Experiment 1. a, In the perturbation trial, the cursor shift location was manipulated from 1 cm to 16 cm from the starting position, while the cursor shift magnitude was fixed at 3 cm. **b,** Temporal profiles of the feedback responses (FBRs) in Experiment 1, aligned to movement onset. **c,** FBRs emerged with a latency of approximately 160 ms relative to movement onset. Latencies were estimated using receiver operating characteristic (ROC) analysis. **d,** Temporal profiles of learning responses (LRs) in Experiment 1. **e-g,** Cross-correlation analysis was used to evaluate temporal similarity and relative timing between FBRs and LRs (**e**). The temporal shift between the FBRs and LRs was defined as the time lag that maximized the individual cross-correlation (**f**), and temporal similarity was quantified as the cross-correlation coefficient at this optimal time lag (**g**). Shaded areas represent the standard error of the mean across participants. Asterisks indicate statistically significant effects (* $p < 0.05$, ** $p < 0.01$, *** $p < 0.001$).

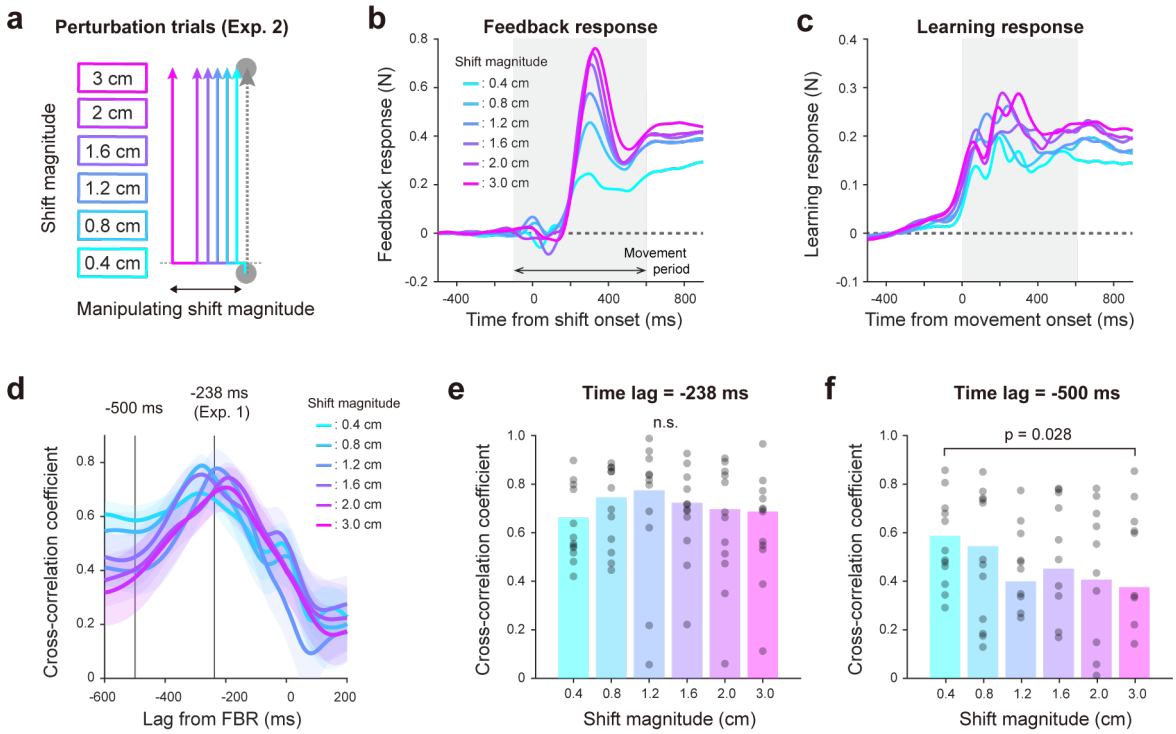

Figure 3: Temporal patterns of feedback and learning responses across different cursor shift magnitudes in Experiment 2. a, In perturbation trials, the shift magnitude was varied from 0.4 cm to 3 cm. **b,** Temporal patterns of the feedback responses (FBRs) in Experiment 2. **c,** Temporal profiles of learning responses (LRs) in Experiment 2. **d,** Cross-correlation analysis between FBRs and LRs used to evaluate their temporal similarity. The plot shows the cross-correlation coefficient as a function of time lag. **e,** Cross-correlation coefficient at the time lag that maximized the average cross-correlation function in Experiment 1 (-238 ms). **f,** Cross-correlation coefficient at a fixed time lag of -500 ms. A significant modulation of correlation coefficients was observed across error magnitudes. Shaded areas represent the standard error of the mean across participants.

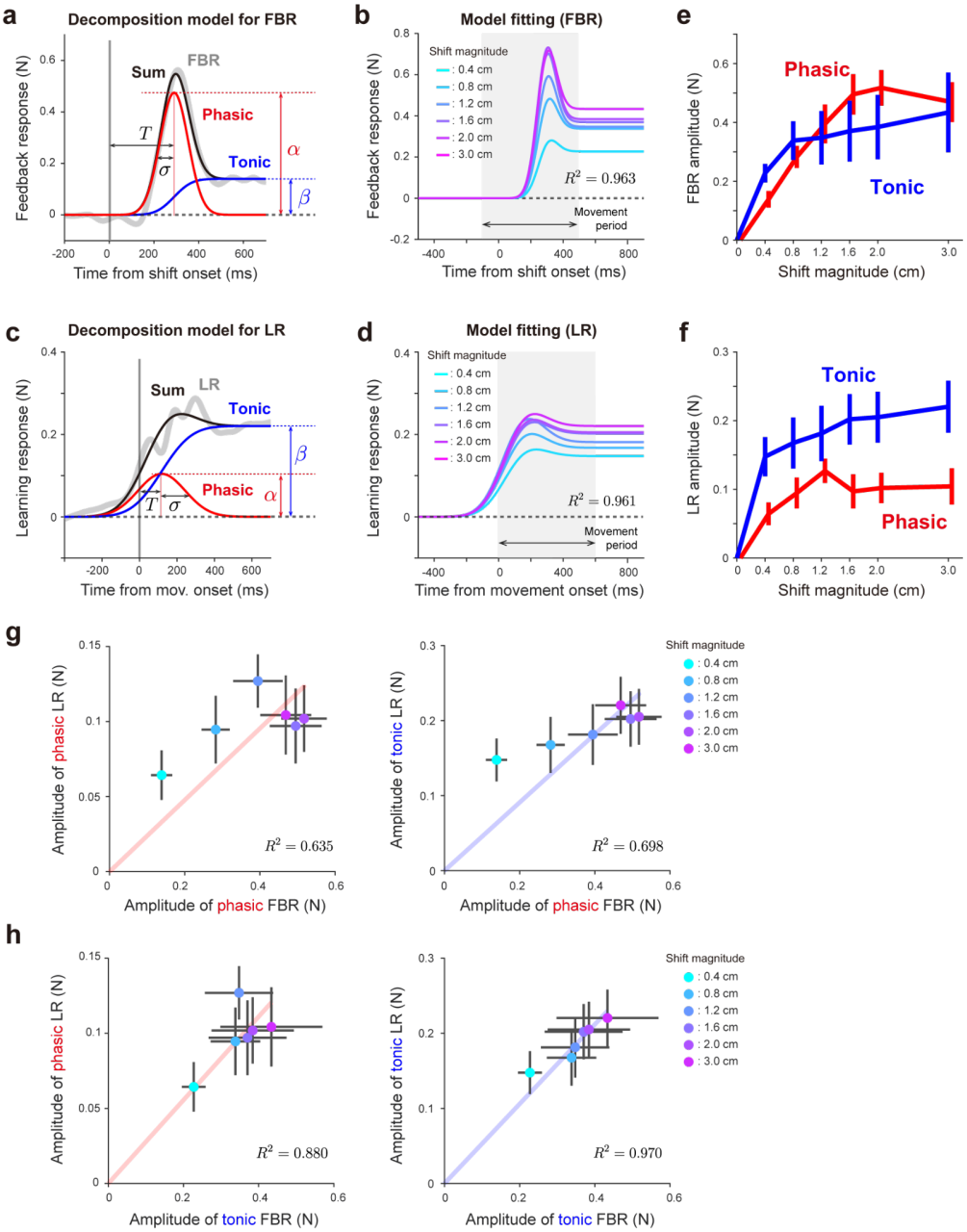

Figure 4: Decomposition of feedback and learning response temporal profiles. a, Temporal profiles of feedback responses (FBRs) were decomposed into two components: an early phasic component and a late tonic component. **b,** Decomposition model reproduced the temporal profiles of FBRs in Experiment 2. **c-d,** The same decomposition procedure was applied to the temporal profiles of the learning responses (LRs). **e,** Modulation of the amplitudes of the phasic and tonic components of the FBR as a function of error magnitude. **f,** Modulation of the amplitudes of the phasic and tonic components of the LR as a function of error magnitude. Error bars represent the standard error of the mean across the participants. **g-h,** Linear regression analyses examining the quantitative relationship between FBRs and LRs using the model $y = ax$, where x represents the amplitude of the phasic (**g**) and tonic components (**h**) of the FBR, and y represents the amplitude of the corresponding phasic (left) and tonic components (right) of the LR. Error bars represent the standard error of the mean across the participants.

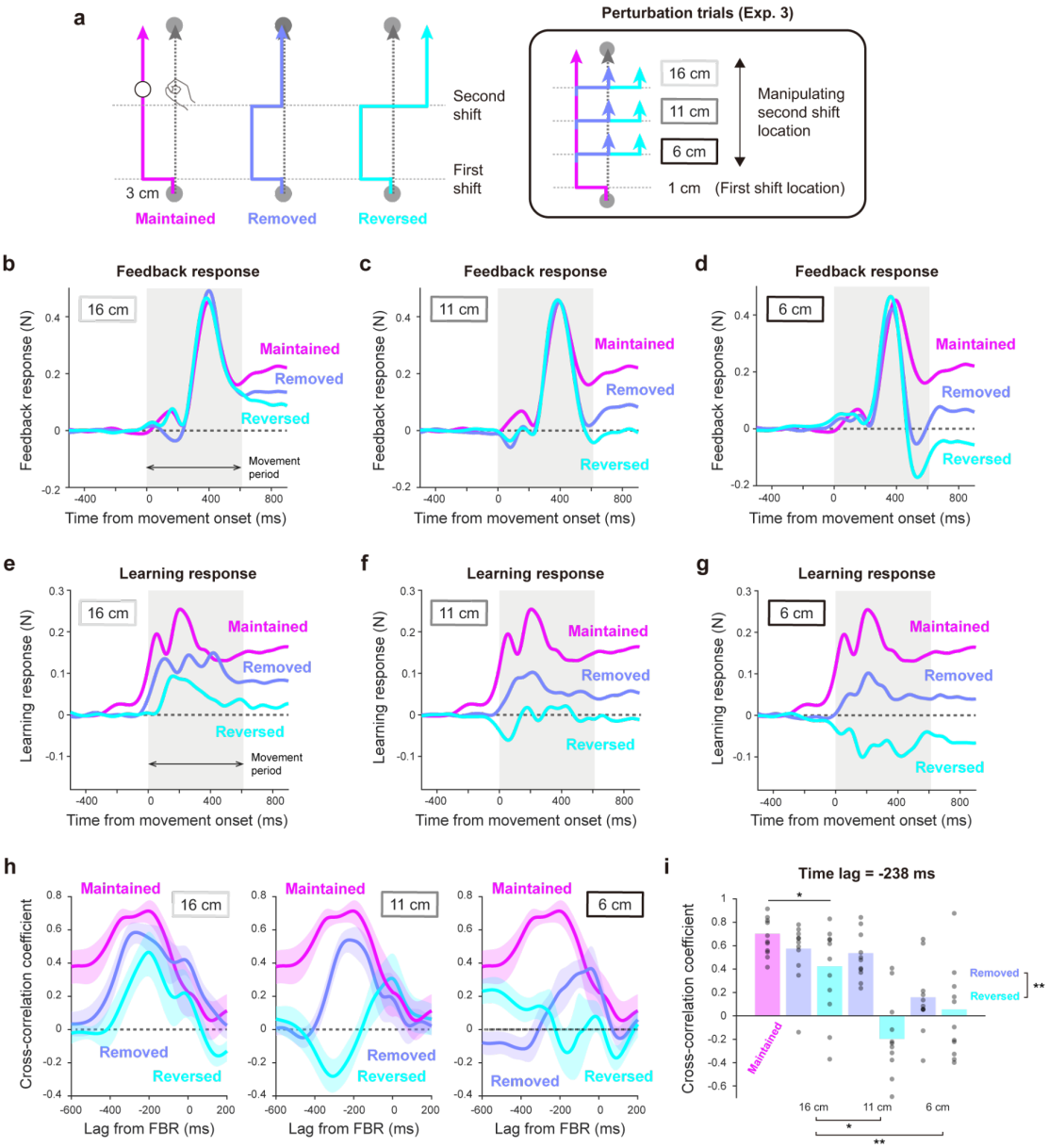

Figure 5: Relationship between the temporal patterns of feedback and learning responses in Experiment 3. a, In perturbation trials, the cursor was shifted laterally twice during a single movement. Three temporal patterns of visual error were tested, and the location of the second shift was varied from 6 cm to 16 cm from the starting position. **b-d,** Temporal profiles of the feedback responses (FBRs) when the second shift occurred at 16 cm (**b**), 11 cm (**c**), and 6 cm (**d**). **e-g,** Temporal patterns of the learning responses (LRs) when the second shift occurred at 16 cm (**e**), 11 cm (**f**), and 6 cm (**g**). **h,** Cross-coefficient function showing the relationship between the cross-correlation coefficient and time lag between FBRs and LRs when the second shift occurred at 16 cm (left), 11 cm (middle), and 6 cm (right). **i,** Cross-correlation coefficient evaluated at the time lag that maximized the cross-correlation function in Experiment 1 (-238 ms). Shaded areas represent the standard error of the mean across participants. Asterisks indicate statistically significant effects (* $p < 0.05$, ** $p < 0.01$, *** $p < 0.001$).

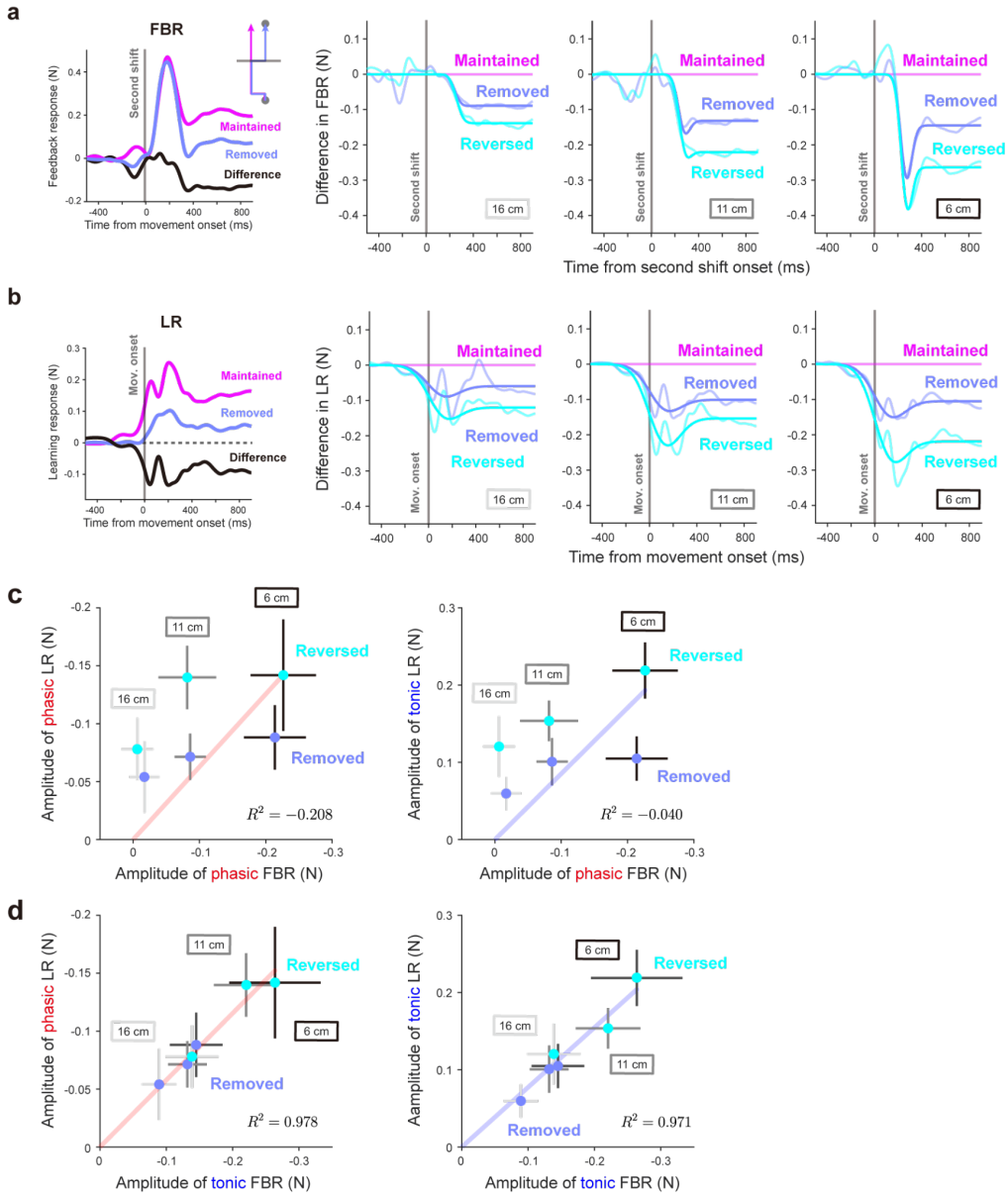

Figure 6: Temporal relationship between feedback and learning responses in Experiment 3. a-b, To isolate the effect of the second cursor shift on feedback (FBRs) and learning responses (LRs), differential force profiles were computed by subtracting the responses in the maintained condition from those in the removed and reversed conditions (insets). The decomposition model successfully reproduced the differential force profiles of the feedback response (**a**) and learning response (**b**) for the second shift when it occurred at 16 cm (left), 11 cm (middle), and 6 cm (right). Solid lines indicate model predictions, and dashed lines indicate experimental data. **c,** Linear regression analysis examining the quantitative relationship between the phasic component of the FBR and the amplitudes of the phasic (left) and tonic (right) components of the LR for the second cursor shift, following the same procedure as in Experiment 2. **d,** Linear regression analysis examining the relationship between the tonic component of the FBR and the amplitudes of the phasic (left) and tonic (right) components of the LR for the second cursor shift. Error bars represent the standard error of the mean across participants.

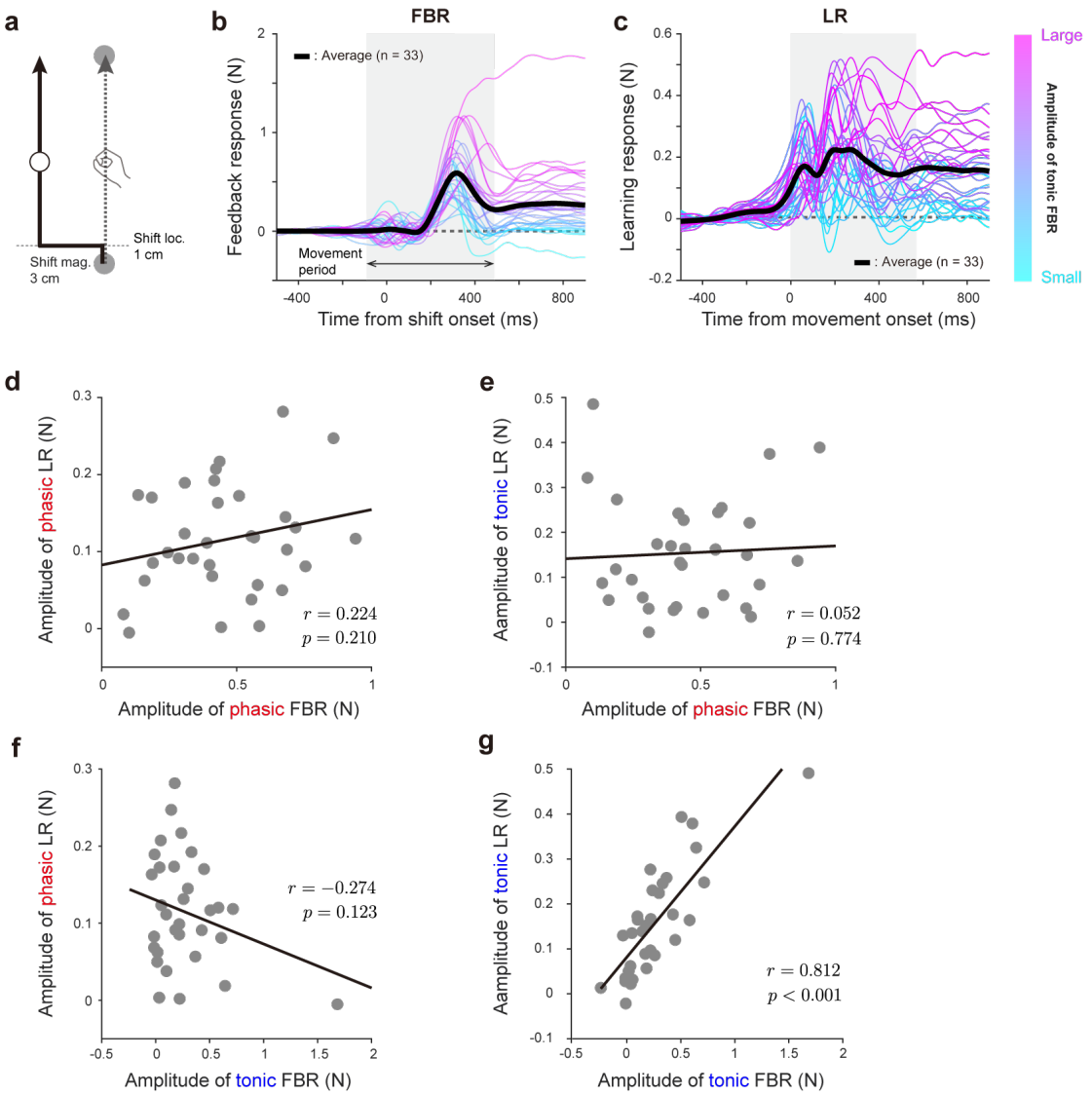

Figure 7: The tonic component of the feedback response explains between-subject variability in learning response amplitude. a, Across Experiments 1–3, all participants experienced an identical temporal pattern of visual error, in which the cursor was shifted laterally by 3 cm at a location 1 cm from the starting position. **b-c**, Temporal profiles of the feedback response (FBR) (**b**) and learning response (LR) (**c**) elicited by this perturbation. Each trace represents an individual participant and the thick black trace represents the average across participants. Participants are ordered according to the amplitude of the tonic component of the FBR, with colors closer to magenta indicating larger tonic feedback responses. **d-g,** Relationships between the amplitudes of the phasic and tonic components of the FBRs and LRs across participants.

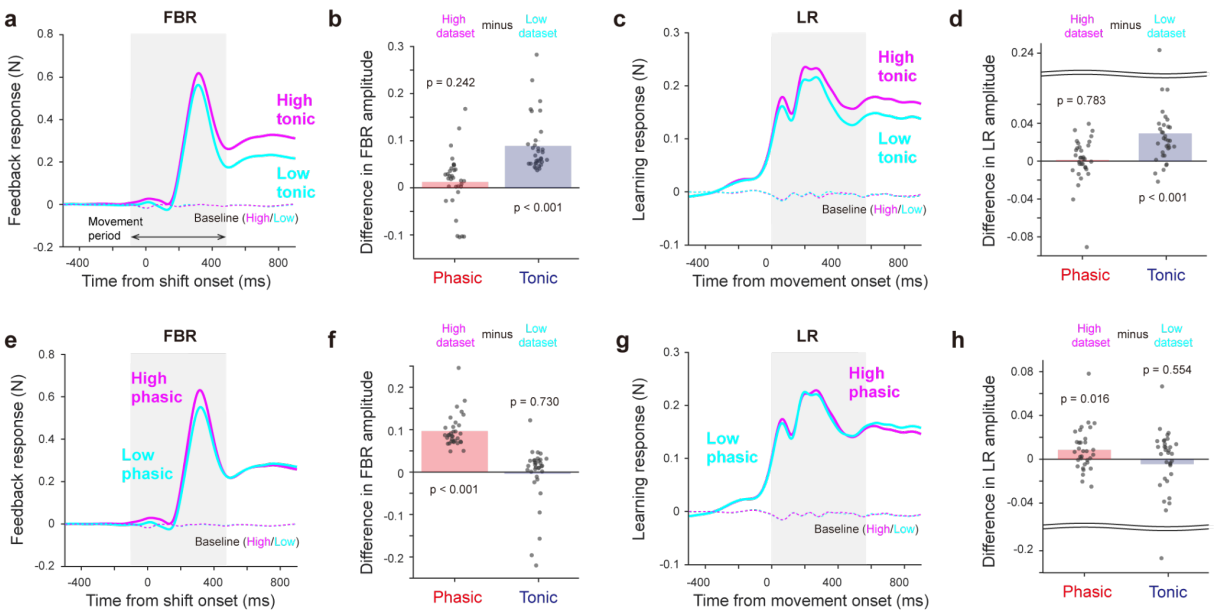

Figure 8: The tonic component of the feedback response explains trial-by-trial variability in learning response amplitude. Trial triplets obtained under an identical cursor shift perturbation (see Fig. 7a) were split into two datasets based on the amplitude of either phasic (**a-d**) and tonic (**e-h**) components of the feedback response (FBR). **a**, Temporal profiles of the FBR for datasets split according to the tonic FBR component and averaged across participants. **b**, Difference in the amplitudes of the phasic and tonic components of the FBR between the High and Low tonic FBR datasets. **c-d**, Temporal profiles (**c**) and difference in the amplitudes of the phasic and tonic components (**d**) of the learning response (LR) for datasets split based on the tonic FBR component. **e,** Temporal profiles of the FBR for the datasets split according to the phasic FBR magnitude. **f,** Amplitudes of the phasic and tonic FBR components for the High- and Low phasic FBR datasets. **g–h,** Temporal profiles (**g**) and component amplitudes (**h**) of the LR for datasets split according to the phasic FBR amplitude.

Supplement Information

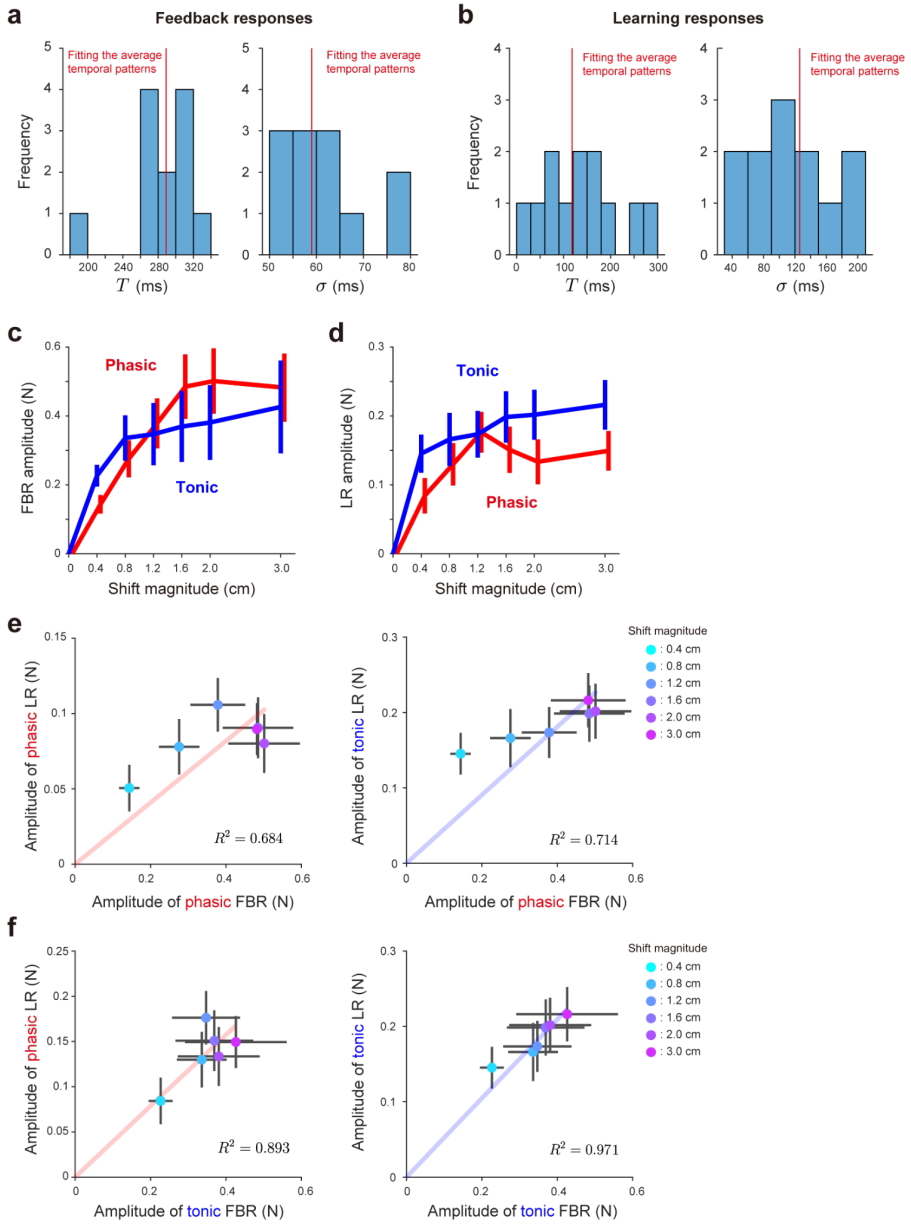

Supplemental Figure 1: Robustness of the quantitative relationship between feedback and learning responses to model parameterization in Experiment 2. Even when additional fitting parameters were introduced for the model (Eq. 1), the quantitative relationship between the feedback response (FBR) and the learning response (LR) remained unchanged. **a-b,** The decomposition model (Eq. 1) was fitted to individual participants' FBRs (**a**) and LRs (**b**) while allowing not only component amplitudes but also onset timing and temporal dispersion to vary as free parameters. The fitted parameter values across participants were distributed around those obtained from the grand-averaged responses. This distribution was relatively narrow for the FBR, indicating high consistency across participants, whereas the LR showed a broader distribution, reflecting greater inter-individual variability. **c-f,** Using this extended fitting procedure, the model successfully reproduced the modulation of FBR and LR amplitudes as a function of visual error magnitude, consistent with the results shown in Fig.4.